



RADIOCARBON AND URANIUM PROFILES IN MARINE GASTROPODS AROUND THE JAPANESE ARCHIPELAGO

Shoko Hirabayashi^{1*}  • Takahiro Aze¹ • Yosuke Miyairi¹ • Hironobu Kan² • Yusuke Yokoyama¹ 

¹Atmosphere and Ocean Research Institute, The University of Tokyo, Kashiwa, Chiba 277-8564, Japan

²Research Center for Coastal Seafloor, Kyushu University, Nishi-ku, Fukuoka 819-0395, Japan

ABSTRACT. In this study, we investigate the distribution of radiocarbon and uranium in the calcified opercula of *Turbo* sp. collected from Ryukyu region and Chiba, Japan, to explore the potential of U/Th dating using mollusks collected from the Japanese archipelago. We acquired high-resolution radiocarbon and uranium concentration measurements using single-stage accelerator mass spectrometry and laser ablation–inductively coupled plasma–mass spectrometry. Our results show that uranium in the opercula of modern *Turbo* sp. is unevenly distributed at concentrations 1000 times less than those in coral skeletons. Radiocarbon found in the calcified opercula samples record ambient seawater radiocarbon values as well as coral skeletons. Uranium in the calcified opercula of Holocene *Turbo marmoratus* were also unevenly distributed and concentrated within the opercula in a different manner than observed in modern samples, suggesting uranium exchange after death. Our results suggest variable uptake of uranium isotopes into mollusk shells and highlights the need for rigorous sample selection criteria when choosing mollusks species for U/Th dating around Japan.

KEYWORDS: gastropods, Radiocarbon, U/Th dating.

INTRODUCTION

High-resolution age determination is a critical and widely used approach in archaeology and paleoclimatology. Radiocarbon (¹⁴C) dating is a powerful tool for determining the ages of samples formed during the past 50,000 years, ¹⁴C ages are required for calibrating calendar ages using IntCal20 for atmospheric samples (Reimer et al. 2020) and Marine20 for marine samples (Heaton et al. 2020). Additionally, when determining ¹⁴C ages of marine samples, it is necessary to consider the age of local marine reservoirs (Alves et al. 2018; Hirabayashi et al. 2019). Datasets relating to local marine reservoir ages are limited and vary with location and time, hindering the accuracy of radiocarbon age determination.

Uranium-thorium (U/Th) dating is another powerful tool used for age determination throughout the Late Quaternary. U/Th dating can obtain a calendar age more than 500,000 years without the calibration required for ¹⁴C dating; however, suitable marine samples for U/Th dating are largely restricted to well-preserved corals, with distributions limited to tropical and temperate regions. Some previous studies have approached the use of U/Th dating with other marine carbonate samples, such as marine mollusks and foraminifera. The uranium abundance in modern and fossil corals is approximately 3 ppm, generally ranging from 2–3.5 ppm (e.g., Broecker 1963; Kaufman et al. 1971; Bard et al. 1990; Edwards et al. 2003). Foraminiferal calcites have reported uranium abundance ranging from 0.02 to 0.05 ppm (Ku 1965; Delaney and Boyle 1983; Russell et al. 1994). For marine mollusks, the corresponding uranium values lie within a range of 10 ppb to 9 ppm (Szabo 1979; Broecker 1963; Edwards et al. 2003). These results imply that uranium concentration differs among species and forms of biogenic aragonite/calcite. Giant clams (*Tridacna gigas*), which live in coral reefs and are used as paleoclimate archives for insolation and sea surface temperature, are often preserved better than fossil corals in terms of their retention of primary aragonite (Ayling et al. 2015). However, uranium concentrations within one modern *Tridacna* specimen have been observed to be

*Corresponding author. Email: s-hirabayashi@aori.u-tokyo.ac.jp

unevenly distributed such that the inner layer was relatively enriched in uranium compared to other layers, such as hinge and outer layers (Ayling et al. 2017).

For closed-system U/Th dating, it is also critical that no uranium uptake and/or loss occurs after death and deposition of organisms. Uranium uptake after death of marine mollusks has been reported although the uranium concentration was evenly distributed in their living shells (Broecker 1963). The uranium distributions in modern and fossil giant clam shells have also been investigated (Nakanishi et al. 1971; Omura and Konishi 1971; Ayling et al. 2017). Using the fission track method, Nakanishi et al. (1971) showed that fossil giant clam shells contain 0.2 ppm and 0.5 ppm of uranium in their inner and outer zones, respectively, while the corresponding values in modern shells were 0.03 ppm and 0.2 ppm. Using laser ablation–inductively coupled plasma–mass spectrometry (LA-ICP-MS), Ayling et al. (2017) reported that uranium concentrations in fossil giant clams of Marine Isotope Stage (MIS) 5e and 11 were different, suggesting that both uranium uptake and loss occurred after death and deposition.

The mechanisms responsible for U/Ca variation in marine bivalve shells also remain unclear. Price and Pearce (1997) studied aragonite marine cockle shells (*Cerastoderma edule*) and related their uranium concentrations to granite weathering and industrial effluents. Gillikin and Dehairs (2013) discussed the relationship between U/Ca ratio in *Saxidomus giganteus* and seawater pH using LA-ICP-MS, concluding that the U/Ca ratio of their aragonite shell was not controlled by environmental factors. Several studies conducting U-series dating have reported strong diagenetic trends in fossil and recent shells (Kaufman et al. 1996, 1971; McLaren and Rowe 1996; Labonne and Hillaire–Marcel 2000); however, these studies were generally conducted at low-resolution and performed limited investigations among of the diverse marine mollusk species.

Some previous studies have suggested that U/Th dating could be applied to marine bivalves. Arslanov et al. (2002) suggested suitable mollusk species in the Caspian, Barents, White, and Black Seas based on comparisons between the ^{14}C and U/Th ages of mollusk shells; it was shown that the ages of the shells calculated by both methods exhibit good agreement up to 15 ka. Cheong et al. (2006) conducted U/Th dating of Holocene mollusks at Jeju Island, Korea. They assumed that the addition of external uranium would not be problematic if mollusks uptaked uranium immediately after deposition and maintained closed systems for both uranium and thorium (Cheong et al. 2006). Rowe et al. (2015) also suggested that U/Th dating could be applied to pre-Holocene mollusk shells because detrital contamination does not appear to be a significant problem in the inner portions of mollusks (*Lithophaga lithophaga*) in the Mediterranean Sea. Nonetheless, a significant age correction is needed for the U/Th age of Holocene *L. lithophaga* shells due to rapid post-mortem uranium uptake (Rowe et al. 2015). These studies investigated limited mollusk species and regions; thus, additional investigation is needed, specific to the Japanese archipelago.

The Japanese archipelago spans a region of subtropical to subarctic waters in the Sea of Japan and the Pacific Ocean (Figure 1). Corals amenable to U/Th dating are distributed only at latitudes below Iki on the Japan Sea side, and Chiba on the Pacific Ocean side. Therefore, most Japanese marine geochronology has relied on ^{14}C dating rather than U/Th dating. However, the number of local marine reservoir ages around Japan is limited. Marine mollusks are common around Japan and it is anticipated that they can provide a paleoclimate archive throughout the Quaternary, although the growth rates of marine mollusks are lower than those of corals. For example, the gastropods *Turbo* sp. are widely distributed from the Ryukyu

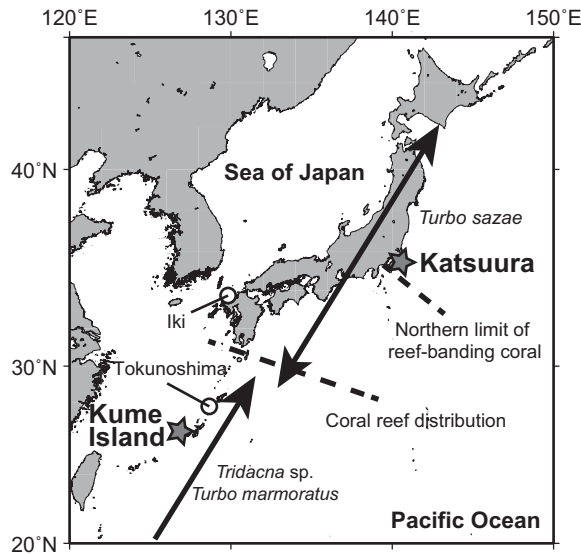


Figure 1 Map showing the distribution of corals and mollusks around Japan and the sampling sites (stars) of the present study at Kume Island and Katsuura. Black arrows show the distribution of *Turbo sazae*, *Turbo marmoratus*, and *Tridacna* sp. around Japan. Dashed line shows the distribution limits of coral reefs and reef-banding corals.

region to the Tohoku region and are an important fisheries resource. Their operculum consists of a thin inner organic layer and an outer calcified (aragonite) layer (Suzuki and Togo 1987). Unlike corals, which feature clear annual bands in their skeletons, it is generally unclear whether marine mollusks, including gastropods, have periodic growth bands or rings that may be used to determine their ages. Giant clam shells and abalones are known to have daily and seasonal growth rings, respectively. *Turbo sazae* has growth bands in its shell and calcified opercula, which are generally related to seawater temperature; however, the bands of Pacific specimens do not exhibit clear periodic cycles related to seasonal seawater temperature variability (Uno 1962; Midorikawa 1986). Hence, the age of such shells is primarily estimated using their height and length.

In this study, we investigate uranium concentrations in modern and fossil calcified opercula of *Turbo* sp., which are widely distributed around Japan, to evaluate their potential for U/Th dating. Understanding uranium incorporation into gastropod shells may also help refine the application of U-series dating of mollusk shells, which could provide an archive with unprecedented resolution for samples older than the range permissible for ^{14}C dating. We also measured ^{14}C concentrations in modern calcified opercula of *Turbo* sp. to evaluate their assumed ages.

MATERIALS AND METHODS

Living and fossil *Turbo* sp. were collected at Ahra beach and Nishimezaki, Kume Island, Japan, in 2018 and 2019. Groundwater discharge that occurs at Ahra beach. Nishimezaki is formed by an uplifted Holocene coral terrace (Kan et al. 1991). Living *Turbo sazae* were collected in Katsuura, Chiba in May 2019. Surface seawater was also collected in September 2019 at Kume Island. The calcified opercula of *Turbo* sp. were polished to obtain flat surfaces, then sliced to compare the difference of the uranium distribution at the surface and through a

transect of calcified opercula. During polishing of the calcified opercula, the thin-brown organic matrix at the surface of both modern and fossil samples disappeared. Samples were cleaned using ultra-pure water and an ultrasonic probe to remove surface contaminants, then dried overnight in an oven at 40°C prior to analysis. LA-ICP-MS analyses were performed at the Atmosphere and Ocean Research Institute, the University of Tokyo, Japan, with a sector field ICP-MS (ELEMENT XR, Thermo Fisher Scientific, Bremen, Germany) equipped with an ArF excimer laser (193 nm) (RESOLUTION M-50 LR, Resonetics) (Kawakubo et al. 2014). The laser was operated at a 5 Hz pulse rate with an applied energy density of $\sim 7 \text{ J/cm}^2$ to the sample surface. We used a circular beam for opercula analysis along the lines shown in Figure S1; the diameter of the ablation spot was set to a size of 155 μm .

Following LA-ICP-MS measurements, living shells and opercula samples were subsampled along their growth bands for radiocarbon dating. Approximately 1–5 mg of powdered samples of shells and opercula were graphitized for radiocarbon dating following the method described by Yokoyama et al. (2010). For fossil samples, approximately 10 mg was collected, and the age determination method of Yokoyama et al. (2007) was employed. The graphite target samples were then analyzed with a single-stage accelerator mass spectrometer (YS-AMS; Yokoyama et al. 2019) at the Atmosphere and Ocean Research Institute, the University of Tokyo, Japan. The ^{14}C age of our Holocene samples were calibrated using OxCal version 4.4 (Bronk Ramsey 1995) via comparison with Marine20 data (Heaton et al. 2020). The ΔR value was assigned as follows: $\Delta\text{R} = -177 \pm 67$, i.e., the calculated weighted mean of ΔR in Kikai Island and Ishigaki Island reported from Hirabayashi et al. (2017) with Marine20 using the CALIB Marine reservoir correction database (available online at <http://calib.org/marine/>) (Reimer and Reimer 2017).

RESULTS AND DISCUSSIONS

Age Determination of Modern Opercula of *Turbo* sp.

Age determination of *Turbo* sp. using the growth rings of calcified opercula is difficult because they lack clear periodic cycles in their rings that can be related to seawater temperature. We measured Mg/Ca and Sr/Ca ratios in calcified opercula of *Turbo* sp. but could not recognize any clear seasonal cycles (Figure S4) such as coral skeletal Sr/Ca (Hirabayashi et al. 2013; Zeng et al. 2022). Hence, the age assumptions of KTN-1 and K-HATE-1 were based on relationships between shell height and age.

We used modern and fossil calcified opercula, rather than shells, for age determinations. This approach requires that we first calculate their shell height/length based on the maximum calcified opercula lengths. Linear regressions comparing shell height/length, and maximum length of calcified opercula have been reported by Kinoshita (2007) for *Turbo marmoratus* and Uno (1962) and Fujii (1998) for *Turbo sazae* (Figures S2 and S3). Kinoshita (2007) reported a linear relationship between shell height and maximum length of calcified opercula in *Turbo marmoratus* from the Amami Islands and Ryukyu Islands. Likewise, Uno (1962) and Fujii (1998) reported a linear relationship for *Turbo sazae*. For modern samples, we used pairs of shells and their opercula to confirm that these samples fit the linear regression lines of Kinoshita (2007), Uno (1962), and Fujii (1998) (Figures S2a and S3a). Subsequently, we estimated calcified opercula lengths for each subsampling band used for radiocarbon dating based on imagery. Using the estimated opercula lengths in the subsampled bands, we calculated the shell height/length of these bands at their time of formation based on the linear regression lines of Kinoshita (2007), Uno (1962), and Fujii (1998).

We then estimated the ages at which the subsampling bands were formed using the relationships between shell height/length and age of *Turbo marmoratus* collected from Tokunoshima Island, the Amami Islands, reported by Igari et al. (2001), and for *Turbo sazae* in Chiba reported by Midorikawa (1986). The results are shown as “expected year” in Table 1. We could not estimate the ages at which the maximum length of a calcified operculum was smaller than 30 mm because of the lack of data in Kinoshita (2007). Both KTN-1 and K-HATE-1 are estimated to have lived for at least three years based on the height and length of their shells. In the following section, we use the expected year of modern samples to compare their ^{14}C variability with seawater radiocarbon data.

Radiocarbon Dating of Opercula of *Turbo* sp.

The ages of fossil calcified opercula of *Turbo* sp. were 871 ± 93 cal year BP for K-ARA-1, 647 ± 79 cal year BP for K-ARA-3 and, 642 ± 80 cal year BP for K-NISH-I. The ^{14}C concentration ($\Delta^{14}\text{C}$ as defined by Stuiver and Polach 1977) of modern calcified opercula of *Turbo sazae* KTN-1 ranges from 14.36‰ to 32.03‰, averaging 21.73‰. The averaged ^{14}C concentration of modern calcified opercula of *Turbo marmoratus*, K-HATE-1, was 32.26‰, ranging from 24.34‰ to 41.25‰.

The ^{14}C concentration (Δ as defined by Stuiver and Polloch 1977) of seawater samples collected at a depth of 10 m in 2019 at Kume Island was 22.03‰. Due to a lack of seawater radiocarbon datasets around the Ryukyu Islands since 2008, we assumed the radiocarbon variability from 2009 to 2019 in the Ryukyu Islands using coral skeletal radiocarbon data reported from Ishigaki Island (Hirabayashi et al. 2017; Yokoyama et al. 2022) and seawater data measured at Kume Island in September 2019 (Table 2) and compared these values with the ^{14}C concentrations recorded in *Turbo* sp. in this study.

As mentioned above, we estimated the radiocarbon ages of each subsample based on the size of modern *Turbo* sp. opercula, using expected ages to calculate Δ and compare with seawater ^{14}C datasets for the Ryukyu Islands (Tables 1 and 2; Figure 2). ^{14}C variability in *Turbo* sp. was found to closely match with seawater ^{14}C , suggesting that ^{14}C in the calcified opercula of *Turbo* sp. reflect the ^{14}C content in ambient seawater; this suggests that our age assumptions for KTN-1 and K-HATE-1 are reasonable. Both *Turbo sazae* and *Turbo marmoratus* ingest marine algae, whose dissolved inorganic carbon reflects ^{14}C variability in ambient seawater (Satoh et al. 2019). Ota et al. (2021) reconstructed ^{14}C variability in Otsuchi Bay based on ^{14}C data recorded in abalone shells, which also ingest marine algae; as such, their shells also reflect ^{14}C variability in ambient seawater. ^{14}C data in KTN-1 were always $\leq 10\%$ higher than those of K-HATE-1, suggesting that differences in the depth and location of the organism’s habitat between Chiba and the Ryukyu Islands have some influence.

Uranium Distribution

Averaged uranium concentrations of modern samples range from 0.003 to 0.115 ppm (Table 3). Our results show that uranium in the opercula of modern *Turbo* sp. were unevenly distributed and that the concentrations recorded are 1000 times less than that measured in coral skeletons (Figure 3), while radiocarbon in opercula samples reflect the radiocarbon values of the ambient seawater as well as corals. The U/Ca ratios of both modern and fossil *Turbo* sp. samples were lower than those of corals and seawater (1.3×10^{-6}) reported by Edwards et al. (2003). U/Ca in

Table 1 Measured radiocarbon data of calcified opercula from living *Turbo* sp.

Sample series	Location (Collection year)	Species	Lab No.	Sample Name	Distance from center/ hinge [mm]	Operculum length [mm]	Length/ Height of the shell [mm]	$\Delta^{14}\text{C}$ [‰]	1 σ	Expected year [CE]	Δ [‰]
KTN-1 series	Katsuura (Collected in May, 2019)	<i>Turbo sazae</i>	YAUT-066513	KTN1-12	0.0			44.78	6.32	2016.35	45.37
			YAUT-066518	KTN1-9(2)	4.5	7.0	15.0	19.02	6.41	2017.03	19.50
			YAUT-066529	KTN1-8	5.2	9.9	22.0	17.86	6.24	2017.29	18.31
			YAUT-066515	KTN1-7	5.5	11.9	27.1	14.36	6.48	2017.48	14.79
			YAUT-066409	KTN1-5(2)	7.4	13.6	31.1	32.03	3.46	2017.63	32.45
			YAUT-066219	KTN1-4	11.4	18.8	44.0	18.52	6.93	2018.10	18.88
			YAUT-066214	KTN1-3	13.8	22.3	52.7	24.94	5.15	2018.42	25.26
			YAUT-066204	KTN1-2	15.4	24.1	57.3	19.08	4.76	2018.59	19.38
			YAUT-066132	KTN1-1	17.0	26.0	61.8	28.06	2.50	2018.76	28.34
K-HATE-1 series	Kume Island (Collected in September, 2019)	<i>Turbo marmoratus</i>	YAUT-067309	K-HATE1-uchi1	0.0			38.20	4.94	2014.84	38.98
			YAUT-066418	K-HATE1-23	3.4			37.36	3.39		
			YAUT-066414	K-HATE1-22	3.9			32.94	3.65		
			YAUT-066428	K-HATE1-21	4.5			37.77	3.51		
			YAUT-066424	K-HATE1-19	5.1			36.33	3.40		
			YAUT-066427	K-HATE1-18	5.7			36.52	3.43		
			YAUT-066425	K-HATE1-17	6.2			36.73	3.44		
			YAUT-066209	K-HATE1-15	9.8			30.94	3.16		
			YAUT-066218	K-HATE1-14	11.4			26.98	6.93		
			YAUT-066206	K-HATE1-13	11.9			27.61	5.56		
			YAUT-066224	K-HATE1-11	12.2	30.9	40.9	24.34	6.36	2017.04	24.84
			YAUT-066225	K-HATE1-10	12.8	33.4	47.3	29.60	5.02	2017.17	30.08
			YAUT-066215	K-HATE1-9	13.6	35.8	53.3	31.70	4.60	2017.29	32.16
			YAUT-066131	K-HATE1-8	17.9	43.8	73.7	41.25	2.52	2017.70	41.66
			YAUT-066226	K-HATE1-7	20.7	48.6	86.1	29.85	7.05	2017.95	30.23
			YAUT-066129	K-HATE1-6	23.6	50.7	91.3	33.89	2.68	2018.06	34.26
			YAUT-066217	K-HATE1-5	25.6	57.1	107.7	25.37	5.28	2018.39	25.69
YAUT-066126	K-HATE1-3	39.2	66.9	132.9	30.88	2.50	2018.90	31.15			
YAUT-066227	K-HATE1-1	40.2	67.6	134.6	24.61	6.96	2018.93	24.87			

Table 2 Measured radiocarbon data of seawater collected at Kume Island in 2019.

Sample series	Location	Lab No.	Sample Name	Depth [m]	$\Delta^{14}\text{C}$ [‰]	1σ	year [CE]	Δ [‰]
Seawater	Kume Island (Collected in September, 2019)	YAUT-050828, YAUT-050839	Kume-sea 1	10	22.11	3.77	2019.67	22.03

modern *Turbo sazae* samples ranges from 10^{-10} to 10^{-6} , while that of *Turbo marmoratus* ranges from 10^{-8} to 10^{-7} . U/Ca ratios in fossil *Turbo sazae* and *Turbo marmoratus* samples were 10^{-7} to 10^{-6} . These results suggest that either biological control or the vital effect of marine gastropods influences uranium incorporation from ambient seawater more strongly than in corals. Based on differences in their U/Ca ratio, the vital effect in *Turbo marmoratus* was possibly stronger than that in *Turbo sazae*, although the number of measurements from which this suggestion is drawn are limited, and more investigation is needed to fully clarify the mechanism responsible for this observation.

In all samples, uranium is most concentrated in the central area, where the age of the organism is likely less than 1 year based on the radiocarbon results discussed above. Uranium was not concentrated into the opercula (more than one year old) of either *Turbo sazae* or *Turbo marmoratus*. The highest uranium values, approximately 2.2 ppm, were recorded in the central regions of the *Turbo sazae* samples, KTN-1 and KTN-5, which are almost the same as the uranium content of corals. Modern *Turbo marmoratus* also contained higher uranium concentrations in the central area than other areas of the opercula, although the highest uranium values in *Turbo marmoratus* were one order of magnitude lower than those in *Turbo sazae* (Table 3).

During the larval stage of *Turbo* sp., the organism adopts a lecithotrophic life mode with a short non-feeding pelagic stage. Shell formation in such non-feeding veligers, including *Turbo sazae*, is thought to be completed in the veliger stage (Onitsuka et al. 2014). Their non-feeding larval stage is usually finished within a few days, after which they settle as juveniles to start feeding on microalgae such as diatoms in the case of *Turbo marmoratus*; and on coralline algae in the case of *Turbo sazae*. Large juveniles and adults feed on the red algae *Gracilaria*, *Hypnea*, and *Echeuma* and brown algae, such as Sargassum. Uranium concentrations in seawater in Ibaraki and Mie were reported as 3.1 ± 0.3 and 2.9 ± 0.3 ng/ml, respectively (Matsuba et al. 2000). Miyake et al. (1970) measured the uranium contents of the open ocean water and in marine algae, showing that concentrations in marine algae were approximately 500–600 ng/g and that the uranium activity ratio in marine algae reflected that of ambient seawater. Ishii et al. (1991) reported uranium distributions in marine organisms, finding higher uranium concentration in soft tissues relative to shells in the case of *Tridacna squamosa*. The highest uranium concentrations of 370 ng/g were identified in the soft tissues of the liver in *Tridacna squamosa*. We therefore propose that the high uranium concentrations recorded in the central opercular regions in modern samples are related to their non-feeding pelagic stage, as opposed to post-settlement. Uranium concentration has not yet been reported in the yolk of the

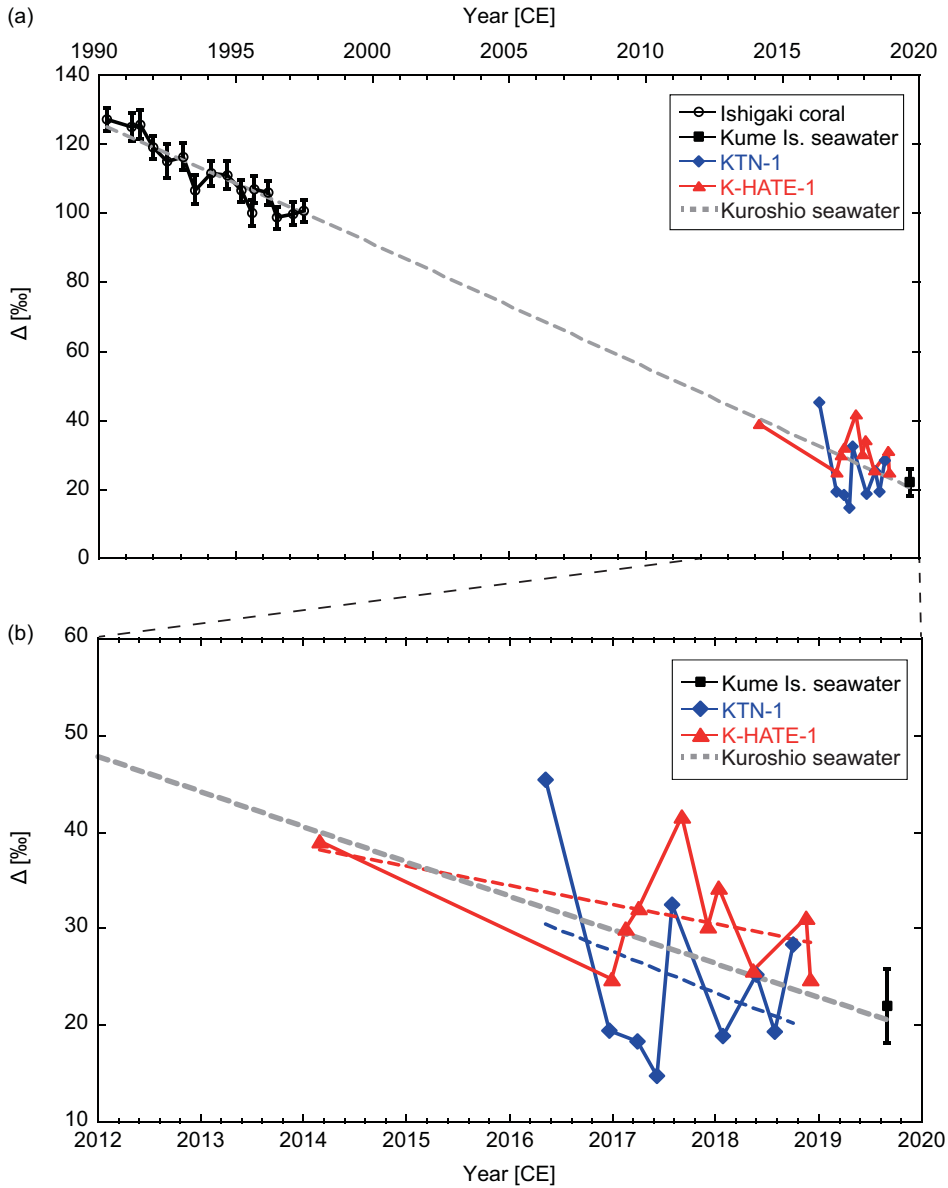


Figure 2 Radiocarbon profile of living *Turbo sazae* (KTN-1, blue) collected from Katsura, living *Turbo marmoratus* (K-HATE-1, red), and seawater at Kume Island (black). The radiocarbon content of Kuroshio seawater was estimated based on coral skeletal radiocarbon data from Ishigaki (Hirabayashi et al. 2017; Yokoyama et al. 2022) and seawater in Kume Island measured in this study.

organism, but it is possible that these concentrations would also be high. Additional investigations will be needed to evaluate this.

The average values of uranium concentrations in all fossil samples were higher than in modern samples. However, the maximum uranium concentration values in fossil samples were lower than modern samples with the exception of *Turbo marmoratus* (Table 3). The highest uranium

Table 3 Measured radiocarbon, U, Mg, Sr, and Ca contents of calcified opercula from *Turbo* sp.

Sample name	Species	Location	Lab No.	Radiocarbon				U/Ca ratio (mmol/mol)		Mg/Ca ratio (mmol/mol)		Sr/Ca ratio (mmol/mol)		U concentration (ppm)		Mg concentration (ppm)		Sr concentration (ppm)		Ca concentration (ppm)	
				¹⁴ C age	1σ	cal BP	1σ	average	max	average	max	average	max	average	max	average	max	average	max	average	max
K-ARA-1	<i>Turbo</i> sp.	Kume Is.	YAUT-066136	1301	21	871	93	1.48.E-04	4.03.E-04	0.969	1.521	1.626	2.163	0.298	0.86	198.64	304.205	1203	1700.8	337696.08	358997.6
K-ARA-1 (Cross section)*	<i>Turbo</i> sp.	Kume Is.	YAUT-066136	1301	21	871	93	1.07.E-04	3.10.E-04	0.901	1.934	1.703	2.686	0.214	0.68	184.68	448.008	1254.2	1945.45	337212.68	413073.1
K-ARA-3	<i>Turbo</i> sp.	Kume Is.	YAUT-066139	1063	21	647	79	1.33.E-04	2.82.E-04	1.060	6.048	1.773	2.579	0.264	0.59	209.8	1075.6	1280.1	1884.88	27331.572	372860.3
K-NISHI	<i>Turbo marmoratus</i>	Kume Is.	YAUT-050928	1056	29	642	80	1.34.E-04	3.58.E-04	1.097	1.698	1.763	2.196	0.230	0.65	190.92	306.006	1050.2	1402.08	286213.09	311620.3
K-HATE-1	<i>Turbo marmoratus</i>	Kume Is.	–	modern	–	–	–	1.20.E-04	1.81.E-04	1.668	3.489	1.988	2.549	0.003	0.11	341.46	729.140	1451.3	1921.2	333964.68	405998.6
KTN-1	<i>Turbo sazae</i>	Katsuura	–	modern	–	–	–	6.05.E-05	1.16.E-03	1.762	3.746	1.898	5.569	0.115	2.23	304.85	688.329	1213.9	3938.31	288525.7	323457.3
KTN-3	<i>Turbo sazae</i>	Katsuura	–	modern	–	–	–	4.78.E-05	5.21.E-04	1.790	4.026	1.700	3.508	0.083	0.92	302.32	645.738	1048.4	2284.35	280769.5	313213.8
KTN-5 (Cross section)	<i>Turbo sazae</i>	Katsuura	–	modern	–	–	–	3.05.E-05	1.03.E-03	2.069	4.155	1.721	5.327	0.063	2.21	438.34	912.663	1310.2	4219.4	347257.53	445329.1

*This sample was cut K-ARA-1 to measure uranium distribution in the cross section of the *Turbo* sp.

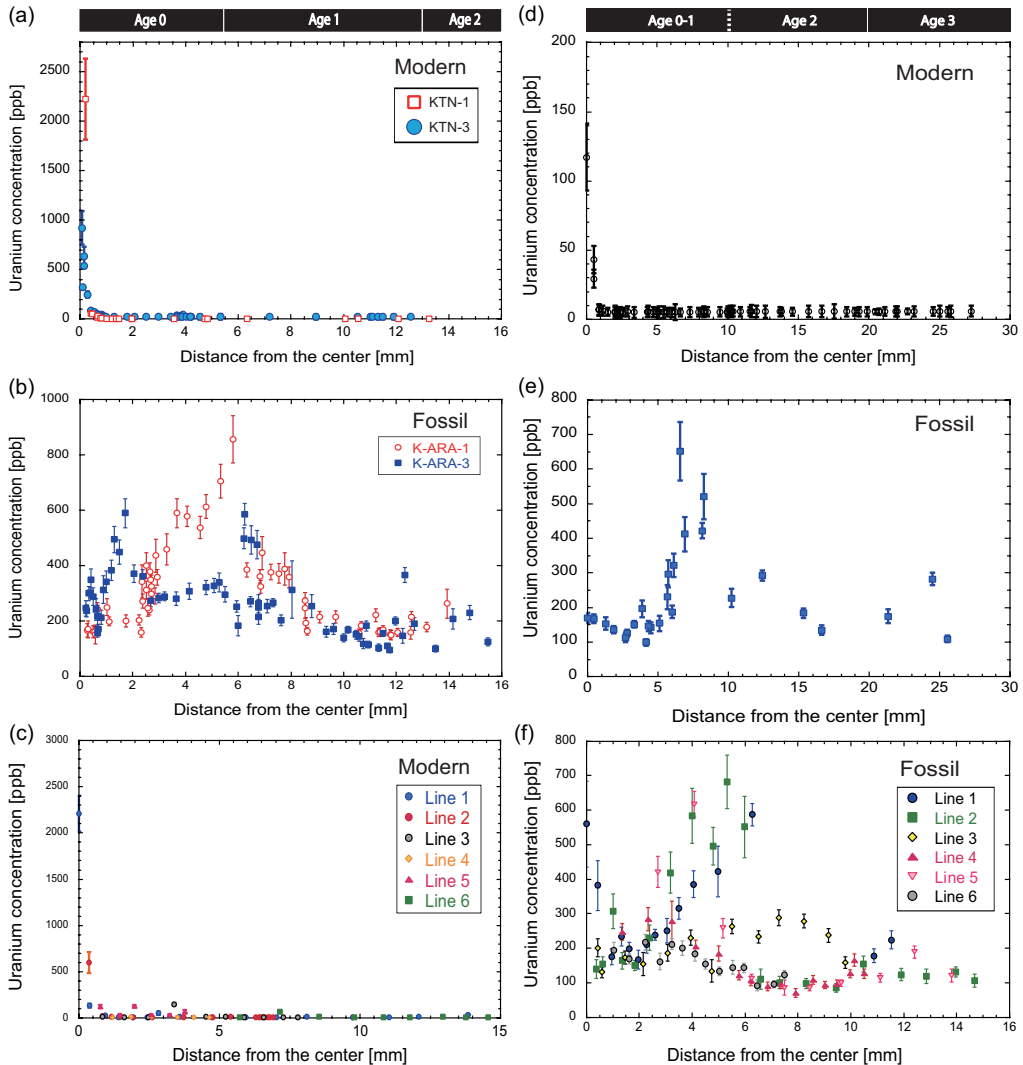


Figure 3 Uranium distributions in calcified opercula of (a) modern *Turbo sazae* samples KTN-1 and KTN-3, (b) fossil *Turbo* sp. samples K-ARA-1 and K-ARA-3, (c) modern *Turbo sazae* sample KTN-5 (cross section), (d) modern *Turbo marmoratus* sample K-HATE-1, (e) fossil *Turbo marmoratus* sample K-NISHI, and (f) fossil *Turbo* sp. sample K-ARA-1 (cross section). Measurement lines are shown in Figure S1.

values in fossil *Turbo sazae* samples were located approximately 5–10 mm from the center, which differs from modern samples (Figure 3). Likewise, the highest uranium concentrations in fossil *Turbo marmoratus* were also located 5–10 mm from the center (Figure 3e). These results suggest that uranium uptake occurred especially in the area of ~5 mm outside from the center, with subsequent uranium loss from the central opercular area after the organism's death and deposition.

Alying et al. (2017) measured uranium concentrations in modern and fossil *Tridacna gigas* samples from MIS 5e and MIS 11 using LA-ICP-MS, showing that uranium uptake occurred mostly in the outer zones of the fossils. Additionally, Alying et al. (2017) developed simple

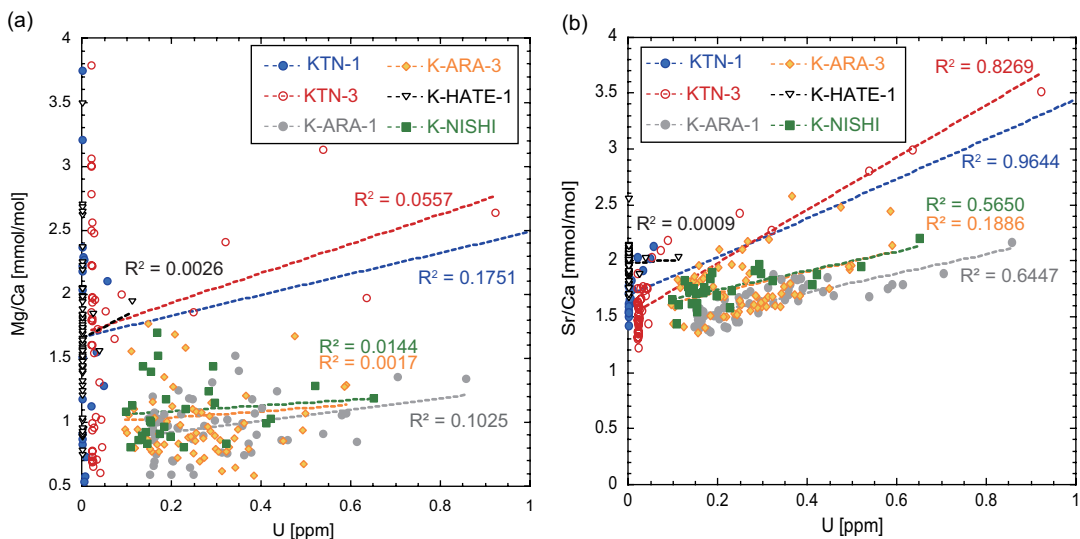


Figure 4 Relationship between uranium concentrations and (a) Mg/Ca and (b) Sr/Ca ratios in modern and fossil *Turbo* sp. measured using laser-ablation-inductively coupled plasma-mass spectrometry (LA-ICP-MS).

uranium uptake and loss models for *T. gigas*, suggesting that uranium adsorption occurred within the first 200,000 years after death and that loss occurred after 50,000 years. In case of two *Turbo sazae* samples, K-ARA-1 and K-ARA-3, the areas with the highest uranium values differ although their age difference is only 230 years. In the case of K-ARA-3, areas with high uranium concentrations were 1.5 mm and 6 mm from the center; for K-ARA-1, this concentrated region was 2–6 mm from the center. These differences might reflect uranium uptake and loss processes in the opercula of *Turbo sazae* during the aforementioned 230-year period. Older fossil *Turbo* sp. samples are required to fully investigate uranium input and output processes over time.

Considering other elements, such as Sr, Mg, and Ca measured simultaneously with U by LA-ICP-MS (Figure S4), we found no correlation between U and Mg/Ca either in the modern or fossil samples (Figure 4a). Unlike U, concentrations of Sr and Mg in fossil and modern samples did not significantly change. Because calcic opercula of *Turbo* sp. consist of aragonite, Mg/Ca ratio would be increased if their opercula underwent diagenesis. Distribution profiles of U/Ca ratios in the fossil calcified opercula was different from that observed for Mg/Ca ratio (Figure S4), suggests that heterogenous uranium distribution in fossil samples did not result from diagenesis. We also observed crystals of modern and fossil samples using scanning electron microscopy–energy dispersive X-ray spectroscopy (SEM-EDS) (Figure S5, Figure S6, Figure S7). We did not identify any recrystallization at the surface of fossil *Turbo marmoratus*. Alying et al. (2017) suggested that uranium uptake may be partly controlled by diagenetic changes. We note however, that since the uranium distributions in K-NISHI, KTN-1, and KTN-3 are similar, areas in which uranium was easily adsorbed were not primarily controlled by diagenesis.

Positive correlations were found between U and Sr/Ca in both modern samples and fossil samples with the exception of modern *Turbo marmoratus* (Figure 4b). Elliot et al. (2009) suggested that Sr/Ca ratio in *T. gigas* exhibited no correlations with temperature, growth rate,

and metabolic rate. On the other hand, studies using other species, such as *S. giganteus* and *M. mercenaria*, have suggested that Sr incorporation into the shell was influenced by growth rates (Takesue and van Geen 2004; Gillikin et al. 2005). In case of *Turbo* sp., Sr/Ca in the calcified opercula did not have any correlations with temperature and growth rates judging from the similarly heterogeneous distribution of U and Sr.

We estimated the age difference reflected by the heterogeneous distribution of uranium in fossil *Turbo* sp. samples. The U/Th ages were determined using following equation (Edwards et al. 1987):

$$\left[\frac{{}^{230}\text{Th}}{{}^{238}\text{U}} \right]_{\text{act}} - 1 = -e^{-\lambda_{230}T} + \frac{\delta^{234}\text{U}_m}{1000} \left(\frac{\lambda_{230}}{\lambda_{230} - \lambda_{234}} \right) (1 - e^{-(\lambda_{230} - \lambda_{234})T}) \quad (1)$$

$$\delta^{234}\text{U} = \left(\left[\frac{{}^{234}\text{U}}{{}^{238}\text{U}} \right]_{\text{act}} - 1 \right) \times 1000 \text{ (‰)} \quad (2)$$

$$\delta^{234}\text{U}_m = \delta^{234}\text{U}_i e^{-\lambda_{234}T} \quad (3)$$

where T is sample age, $[{}^{230}\text{Th}/{}^{238}\text{U}]_{\text{act}}$ and $[{}^{234}\text{U}/{}^{238}\text{U}]_{\text{act}}$ are the activity ratios for each isotope, and λ_{230} and λ_{234} are the decay constants for ${}^{230}\text{Th}$ and ${}^{234}\text{U}$, respectively. We used decay constants of $\lambda_{230} = 9.1705 \times 10^{-6} \text{ year}^{-1}$ and $2.82206 \times 10^{-6} \text{ year}^{-1}$ as reported by Cheng et al. (2013). $\delta^{234}\text{U}_m$ is the uranium isotope ratios corresponding to the time at which U/Th was measured and $\delta^{234}\text{U}_i$ is the initial value. We assumed a constant ${}^{230}\text{Th}$ concentration in the calcified opercula of *Turbo* sp. and that ${}^{234}\text{U}/{}^{238}\text{U}$ in the calcified opercula of *Turbo* sp. was as same as that of seawater. Therefore, we used a $\delta^{234}\text{U}_{\text{initial}}$ of 146.8 following Andersen et al. (2010) and calculated $\delta^{234}\text{U}_m$ using Eq. (3) for each fossil sample. We calculated ${}^{230}\text{Th}$ concentrations using Eq. (1) with the minimum ${}^{238}\text{U}$ concentrations in each fossil sample. We used calibrated ${}^{14}\text{C}$ ages using Marine20 shown in Table 3 as the value of T in Eq. (1). After evaluating the ${}^{230}\text{Th}$ concentration, we calculated U/Th ages using the maximum ${}^{238}\text{U}$ values in each sample and the estimated ${}^{230}\text{Th}$. The age differences were found to be 800 years, 602 years, and 605 years in KTN-1, KTN-3, and K-NISHI, respectively (Table S1). Although some assumption were made in determining the distribution of ${}^{230}\text{Th}$ and $\delta^{234}\text{U}$ in the calcified opercula of *Turbo* sp., our estimations suggest that uranium uptake and loss processes should be considered when using fossil marine mollusks for U/Th dating. Contrary to Arslanov et al. (2002) and Cheong et al. (2006), who suggested that U/Th dating may be performed using Holocene samples, our results warn against using Holocene *Turbo* sp. samples from the Japanese archipelago for U/Th dating without careful scrutiny.

CONCLUSION

We measured radiocarbon and uranium concentrations in modern and fossil *Turbo* sp. collected from Chiba and Kume Island, Japan. Although radiocarbon in the calcified opercula of modern samples seems to record ${}^{14}\text{C}$ of ambient seawater, as corals, uranium concentrations in calcified opercula were a small fraction (1/1000) of the uranium concentrations found in corals. Uranium distributions in opercula are heterogeneous and concentrations can reach ppm levels in the center of the opercula; where localized values may be as high as those observed in corals. These results suggest that uranium from the ingestion of marine algae by juvenile and adult mollusks is not efficiently incorporated into their shells; on the other hand, uranium is readily

absorbed during the planktonic growth stage. The uranium distribution in fossil *Turbo* sp. was also found to be heterogeneous, but the areas exhibiting the highest uranium concentration were slightly different from those of the modern samples. Uranium distributions in fossil samples can affect U/Th ages by up to 800 years in case of 1 ka-old samples. Our study indicates that uranium uptake and loss even occur in Holocene-age marine mollusks, and can inhibit accurate U/Th dating using *Turbo* sp. Thus, further investigation is needed to understand the criteria for choosing appropriate mollusks species for U/Th dating around the Japanese archipelago.

ACKNOWLEDGMENTS

We thank constructive comments from Dr. Derek Hamilton and an anonymous reviewer that improved the manuscript. Isamu Nakayoshi and Arisa Izeki supported this study by collecting our samples in Kume Island. This study was financially supported by JSPS Grant-in-Aid for Young Scientists (19K14805), and Grant-in-Aid for Scientific Research S (16H06309).

SUPPLEMENTARY MATERIAL

To view supplementary material for this article, please visit <https://doi.org/10.1017/RDC.2023.122>

REFERENCES

- Alves EQ, Macario K, Ascough P, Ramsey BC. 2018. The worldwide marine radiocarbon reservoir effect: Definitions, mechanisms, and prospects. *Reviews of Geophysics* 56(1):278–305.
- Andersen MB, Stirling CH, Zimmermann B, Halliday AN. 2010. Precise determination of the open ocean $^{234}\text{U}/^{238}\text{U}$ composition. *Geochemistry, Geophysics, Geosystems* 11(12):Q12003.
- Arslanov KhA, Tertychny NI, Kuznetsov VY, Chernov SB, Lokshin NV, Gerasimova SA, Maksimov FE, Dodonov AE. 2002. $^{230}\text{Th}/\text{U}$ and ^{14}C dating of mollusc shells from the coasts of the caspian, barents, white and black seas. *Geochronometria* 21:49–56.
- Ayling BF, Chappell J, Gagan MK, McCulloch MT. 2015. ENSO variability during MIS 11 (424–374 ka) from *Tridacna gigas* at Huon Peninsula, Papua New Guinea. *Earth and Planetary Science Letters* 431:236–246.
- Ayling BF, Eggins S, McCulloch MT, Chappell J, Grün R, Mortimer G. 2017. Uranium uptake history, open-system behaviour and uranium-series ages of fossil *Tridacna gigas* from Huon Peninsula, Papua New Guinea. *Geochimica et Cosmochimica Acta* 213:475–501.
- Bard E, Hamelin B, Fairbanks RG, Zindler A. 1990. Calibration of the ^{14}C timescale over the past 30,000 years using mass spectrometric U-Th ages from Barbados corals. *Nature* 345(6274):405–410.
- Broecker WS. 1963. A preliminary evaluation of uranium series inequilibrium as a tool for absolute age measurement on marine carbonates. *Journal of Geophysical Research* 68(9): 2817–2834.
- Cheng H, Edwards RL, Shen C-C, Polyak VJ, Asmerom Y, Woodhead J, Hellstrom J, Wang Y, Kong X, Spötl C, Wang X, Alexander Jr. EC. 2013. Improvements in ^{230}Th dating, ^{230}Th and ^{234}U half-life values, and U-Th isotopic measurements by multi-collector inductively coupled plasma mass spectrometry. *Earth and Planetary Science Letters* 371–372:82–91.
- Cheong C-S, Choi MS, Kim BK, Sohn YK, Kwon ST. 2006. $^{230}\text{Th}/^{234}\text{U}$ dating of Holocene mollusk shells from Jeju Island, Korea, by multiple collectors inductively coupled plasma mass spectrometry. *Geosciences Journal* 10(1):67–74.
- Delaney ML, Boyle EA. 1983. Uranium and thorium isotope concentrations in foraminiferal calcite. *Earth and Planetary Science Letters* 62(2): 58–262.
- Edwards RL, Chen JH, Wasserburg GJ. 1987. ^{238}U - ^{234}U - ^{230}Th - ^{232}Th systematics and the precise measurement of time over the past 500,000 years. *Earth and Planetary Science Letters* 81(2–3):175–192.
- Edwards RL, Gallup CD, Cheng H. 2003. Uranium-series dating of marine and lacustrine carbonates. *Uranium. Reviews in Mineralogy and Geochemistry* 52(1):363–405.
- Elliot M, Welsh K, Chilcott C, McCulloch M, Chappell J, Ayling B. 2009. Profiles of trace elements and stable isotopes derived from giant long-lived *Tridacna gigas* bivalves. *Palaeogeography, Palaeoclimatology, Palaeoecology* 280(1–2):132–142.

- Fujii A. 1998. Fisheries biology of the spiny top shell, *Batillus cornutus*, in the coastal waters of Tsushima Island. *Bull Nagasaki Prefect Inst Fish* 24:69–115.
- Gillikin DP, Dehairs F. 2013. Uranium in aragonitic marine bivalve shells. *Palaeogeography, Palaeoclimatology, Palaeoecology* 373:60–65.
- Gillikin DP, Lorrain A, Navez J, Taylor JW, André L, Keppens E, Baeyens W, Dehairs E. 2005. Strong biological controls on Sr/Ca ratios in aragonitic marine bivalve shells. *Geochemistry, Geophysics, Geosystems* 6(5):Q05009.
- Heaton TJ, Köhler P, Butzin M, Bard E, Reimer RW, Austin WEN, Ramsey CB, Grootes PM, Hughen KA, Kromer B, Reimer PJ, Adkins J, Burke A, Cook MS, Olsen J, Skinner LC. 2020. Marine20—the marine radiocarbon age calibration curve (0–55,000 cal BP). *Radiocarbon* 62(4):779–820.
- Hirabayashi S, Yokoyama Y, Suzuki A, Esat T, Miyairi Y, Aze T, Siringan F, Maeda Y. 2019. Local marine reservoir age variability at Luzon Strait in the South China Sea during the Holocene. *Nuclear Instruments and Methods in Physics Research Section B* 455:171–177.
- Hirabayashi S, Yokoyama Y, Suzuki A, Kawakubo Y, Miyairi Y, Okai T, Nojima S. 2013. Coral growth-rate insensitive Sr/Ca as a robust temperature recorder at the extreme latitudinal limits of Porites. *Geochemical Journal* 47(3):e1–e5.
- Hirabayashi S, Yokoyama Y, Suzuki A, Miyairi Y, Aze T. 2017. Multidecadal oceanographic changes in the western Pacific detected through high-resolution bomb-derived radiocarbon measurements on corals: western Pacific oceanography and bomb ¹⁴C. *Geochemistry, Geophysics, Geosystems* 18(4):1608–1617.
- Hirabayashi S, Yokoyama Y, Suzuki A, Miyairi Y, Aze T. 2017. Short-term fluctuations in regional radiocarbon reservoir age recorded in coral skeletons from the Ryukyu Islands in the north-western Pacific: short-term fluctuations in local reservoir age in the Ryukyus. *Journal of Quaternary Science* 32(1):1–6.
- Igari T, Matsumoto N, Kitaue K. 2001. Growth of the Juvenile green snail, *Turbo marmoratus* in Tokunoshima Island, Kagoshima Prefecture. *Suisanzoshoku* 49:413–414.
- Ishii T, Nakahara M, Matsuba M, Ishikawa M. 1991. Determination of ²³⁸U in marine organisms by inductively coupled plasma mass spectrometry. *Nippon Suisan Gakkaishi* 57(5):779–787.
- Kan H, Takahashi T, Koba M. 1991. Morphodynamics on Holocene reef accretion: Drilling results from Nishimezaki reef, Kume Island, the central Ryukyus. *Geographical Review of Japan, Series B* 64(2):114–131.
- Kaufman A, Broecker WS, Ku TL, Thurber DL. 1971. The status of U-series methods of mollusk dating. *Geochimica et Cosmochimica Acta* 35(11):1155–1183.
- Kaufman A, Ghaleb B, Wehmiller JF, Hillaire-Marcel C. 1996. Uranium concentration and isotope ratio profiles within *Mercenaria* shells: Geochronological implications. *Geochimica et Cosmochimica Acta* 60(19):3735–3746.
- Kawakubo Y, Yokoyama Y, Suzuki A, Okai T, Alibert C, Kinsley L, Eggins S. 2014. Precise determination of Sr/Ca by laser ablation ICP-MS compared to ICP-AES and application to multi-century temperate corals. *Geochemical Journal* 48(2):145–152.
- Kinoshita N. 2007. New discussions on shell trade: based on archaeological sites in Amami Oshima from the 6th through 8th centuries with large amounts of excavated shells from Great Green Turban Snails. *Kumamoto Journal of Cult Humanities* 93:1–22.
- Ku TL. 1965. An evaluation of the U234/U238 method as a tool for dating pelagic sediments. *Journal of Geophysical Research* 70(14):3457–3474.
- Labonne M, Hillaire-Marcel C. 2000. Geochemical gradients within modern and fossil shells of *Concholepas* *Concholepas* from northern Chile: an insight into U-Th systematics and diagenetic/ authigenic isotopic imprints in mollusk shells. *Geochimica et Cosmochimica Acta* 64(9):1523–1534.
- Matsuba M, Ishii T, Nakahara M, Nakamura R, Watabe T, Hirano S. 2000. The concentrations of uranium in marine organisms. *Radioisotopes* 49(7):346–353.
- McLaren SJ, Rowe PJ. 1996. The reliability of uranium-series mollusc dates from the western Mediterranean basin. *Quaternary Science Reviews* 15(7):709–717.
- Midorikawa T. 1986. [The knowledge and problems about the turban shell] *Sazae ni kansuru kiou chiken to mondaiten* (in Japanese). *Wasuizoushihou* 17:36–56.
- Miyake Y, Sugimura Y, Mayeda M. 1970. The uranium content and the activity ratio ²³⁴U/²³⁸U in marine organisms and sea water in the western North Pacific. *Journal of Oceanography* 26(3):123–129.
- Nakanishi T, Omura A, Sakanoue M, Konishi K. 1971. Distribution of uranium and sodium in fossil *Tridacna* shell studied through fission track method and activation autoradiography. *Fossils* 21:6–14.
- Omura A, Konishi K. 1971. Isotope content of uranium, thorium and protactinium in present-day and fossil *Tridacna* shells, and its application to chronology. *Fossils* 21:15–27.
- Onitsuka T, Kimura R, Ono T, Takami H, Nojiri Y. 2014. Effects of ocean acidification on the early developmental stages of the horned turban, *Turbo cornutus*. *Marine Biology* 161(5):1127–1138.
- Ota K, Yokoyama Y, Miyairi Y, Hayakawa J, Satoh N, Fukuda H, Tanaka K. 2021. Northeast Pacific seawater radiocarbon recorded in abalone shells

- obtained from Otsuchi Bay, Japan. *Radiocarbon* 63(4):1249–1258.
- Price GD, Pearce NJG. 1997. Biomonitoring of pollution by *Neorastoderma edule* from the British Isles: A Laser ablation ICP-MS study. *Marine Pollution Bulletin* 34(12):1025–1031.
- Ramsey BC. 1995. Radiocarbon calibration and analysis of stratigraphy: the OxCal program. *Radiocarbon* 37(2):425–430.
- Reimer PJ, Austin WEN, Bard E, Bayliss A, Blackwell PG, Bronk Ramsey C, Butzin M, Cheng H, Edwards RL, Friedrich M, et al. 2020. The IntCal20 Northern Hemisphere radiocarbon age calibration curve (0–55 cal kBP). *Radiocarbon* 62(4):725–757.
- Reimer RW, Reimer PJ. 2017. An online application for ΔR calculation. *Radiocarbon* 59(5):1623–1627.
- Rowe PJ, Turner JA, Andrews JE, Leeder MR, van Calsteren P, Thomas L. 2015. Uranium-thorium dating potential of the marine bivalve *Lithophaga lithophaga*. *Uranium. Quaternary Geochronology* 30:80–89.
- Russell AD, Emerson S, Nelson BK, Erez J, Lea DW. 1994. Uranium in foraminiferal calcite as a recorder of seawater uranium concentrations. *Geochimica et Cosmochimica Acta* 58(2): 671–681.
- Satoh N, Fukuda H, Miyairi Y, Yokoyama Y, Nagata T. 2019. Position-dependent radiocarbon content of the macroalgae *Undaria pinnatifida* as an indicator of oceanographic conditions during algal growth. *Journal of Oceanography* 75(4):349–358.
- Stuiver M, Polach HA. 1977. Discussion reporting of ^{14}C data. *Radiocarbon* 19(3):355–363.
- Suzuki S, Togo Y. 1987. Microstructure of the calcified opercula of some Tubind gastropods. Association for the Geological Collaboration in Japan 41:48–56.
- Szabo BJ. 1979. ^{230}Th , ^{231}Pa , and open system dating of fossil corals and shells. *Journal of Geophysical Research* 84(C8):4927.
- Takesue RK, van Geen A. 2004. Mg/Ca, Sr/Ca, and stable isotopes in modern and Holocene *Protothaca staminea* shells from a northern California coastal upwelling region. *Geochimica et Cosmochimica Acta* 68(19):3845–3861.
- Uno Y. 1962. Studies on the aquaculture of *Turbo cornutus*–Solander with special reference to the ecology and periodicity of the growth. *Journal of the Tokyo University of Fisheries* 6:1–76.
- Yokoyama Y, Koizumi M, Matsuzaki H, Miyairi Y, Ohkouchi N. 2010. Developing ultra small-scale radiocarbon sample measurement at the University of Tokyo. *Radiocarbon* 52(2): 310–318.
- Yokoyama Y, Miyairi Y, Aze T, Yamane M, Sawada C, Ando Y, de Natris M, Hirabayashi S, Ishiwa T, Sato N, Fukuyo N. 2019. A single stage accelerator Mass Spectrometry at the Atmosphere and Ocean Research Institute, The University of Tokyo. *Nuclear Instruments and Methods in Physics Research Section B* 455:311–316.
- Yokoyama Y, Miyairi Y, Matsuzaki H, Tsunomori F. 2007. Relation between acid dissolution time in the vacuum test tube and time required for graphitization for AMS target preparation. *Nuclear Instruments and Methods in Physics Research Section B* 259(1):330–334.
- Yokoyama Y, Tims S, Froehlich M, Hirabayashi S, Aze T, Fifield LK, Koll D, Miyairi Y, Pavetich S, Kuwae M. 2022. Plutonium isotopes in the North Western Pacific sediments coupled with radiocarbon in corals recording precise timing of the Anthropocene. *Scientific Reports* 12(1):10068.
- Zeng Y, Yokoyama Y, Hirabayashi S, Miyairi Y, Suzuki A, Aze T, Kawakubo Y. 2022. A rapid and precise method of establishing age model for coral skeletal radiocarbon to study surface oceanography using coupled X-ray photos and ICP-AES measurement. *Nuclear Instruments and Methods in Physics Research Section B* 533:23–28.